Vol. 6, No. 1, Spring 2021, pp. 1-10
دوره ششم، شماره ۱، بهار ۱۴۰۰، صفحه ۱ تا ۱۰

نشریه مهندسی منابع معدنی
Journal of Mineral Resources Engineering
(JMRE)

DOI:10.30479/jmre.2020.13245.1409

Research Paper

Discrimination Between Hypogene and Enriched Supergene Zones Using Fractal and Sequential Factor Analysis in Milloieh Porphyry Copper Deposit, SE Iran

Ahmadi N.R.[1], Jafari M.R.[2*], Espahbod M.R.[3], Kohansal Ghadimvand N.[2]

1- Ph.D Student, Dept. of Geology, North Tehran Branch, Islamic Azad University, Tehran, Iran
2- Assistant Professor, Dept. of Geology, North Tehran Branch, Islamic Azad University, Tehran, Iran
3- Associate Professor, Dept. of Geology, North Tehran Branch, Islamic Azad University, Tehran, Iran

(Received: 11 May 2020, Accepted: 24 Jun. 2020)

Abstract

The aim of this study was to separate the different mineralized zones consisting of supergene enrichment and hypogene zones in Milloieh porphyry Cu deposit (SE Iran) based on subsurface data and using the Staged Factor Analysis (SFA) and Concentration-Number (C-N) fractal modelling. Results obtained by SFA indicate that Cu and Mo were situated in a factor as F2-2 which was modelled by the C-N fractal method for separation of the mineralized zones. The supergene enrichment zone derived via the SFA and C-N fractal analysis contains 0.86% for Cu and 5.3 ppm for Mo. Moreover, the hypogene zone obtained by this modelling has Cu and Mo average values of 0.59% and 1.88 ppm, respectively. These mineralized zones were correlated with mineralographical data obtained by the polished section microscopic studies which indicate that the obtained zones based on the SFA and C-N fractal model are consistent with the geological and mineralization data.

Keywords

Staged Factor Analysis (SFA), Concentration-Number (C-N) fractal modelling, Milloieh porphyry.

Corresponding Author, Email: mr_jaafari@iut-tnb.ac.ir

1- INTRODUCTION

Porphyry copper deposits are the main resource of copper all around the world. This deposits' type is the most important, because of wide reserves of precious metals such as molybdenum and gold together with copper. One of the essential studies on the porphyry deposits is identifying mineralized zones particularly supergene enrichment and hypogene zones [1]. Conventional geological methods for detection and recognition of zones in the porphyry deposits are based on mineralographical and petrographical studies [1-4]. However, statistical analysis and mathematical methods have been utilized to distinguish mineralized zones since the 1950s [5-8]. The main aim of statistical analysis particularly factor analysis is to extract a few 'factors' to raise ability of illustrating multivariate data [9-13]. Staged Factor Analysis (SFA) is one of multivariate statistical techniques which can reduce variables (elements) and define paragenetic elements in different factors [13]. Fractal/multifractal modelling have widely been used in the mineral exploration and economic geology [14-19]. Several fractal models have been developed and proposed in geochemical exploration to separate geochemical populations, e.g., Concentration-Area (C-A) [20], Concentration-Distance (C-D) [10], Number-Size (N-S) [21], Concentration-Volume (C-V) [7] and Concentration-Number [22] based on exploratory data. In this paper, the SFA is used for reducing factor and defining paragenesis factor for Cu and Mo and used the C-N fractal model for separation of different mineralized zones in Milloieh porphyry deposit, SE Iran, and the results are correlated with the geological data.

2- METHODOLOGY

2-1- SFA

Multivariate statistical methods such as factor analysis supposes that data have normal distribution; however, geochemical exploration data never demonstrate a normal distribution [23,24]. The accuracy of the measurements changes with element concentration; values are less accurate at very low and high concentrations [25]. In this paper, the Napierian logarithm (Ln; logarithmic basement Napierian digit) is used for transforming values of multivariate geochemical data in a classical factor analysis by SPSS software. There are rock samples data from core analysis and these are not close data such as stream sediments. After transformation of geochemical data, standard techniques such as classical estimation of correlation matrix were used to find relationship between all the variables [26]. The major purpose of the factor analysis is to realize a few and common factors from multivariate data [27]. Principal component analysis (PCA) is used to extract principal components for identifying hidden multivariate data structures and decreasing the number of variables [28-30]. The SFA consists of two main phases as follows:

The first phase is for extraction of 'clean' factors and the second phase is for extraction of a significant multi-element zonation signature of the mineral deposit-type sought to calculate reliable loadings and factor scores. Each of the main phases of the SFA may comprise sub-phases depending on geochemical data and the mineral deposit-type sought [29,30].

2-2- C-N Fractal Modeling

Hassanpour and Afzal [22] proposed the C-N fractal model for delineation of mineralized zones and barren host rocks in porphyry Cu deposits, this model can be expressed as Equation 1:

$$N(\geq\rho) \propto \rho^{-\beta} \qquad (1)$$

where:

$N(\geq\rho)$: shows the sample number with concentration values greater than the ρ value,

ρ: concentration of element,

β: fractal dimension.

In this method geochemical data has not undergone pre-treatment and evaluation [17]. The C-N fractal model was carried out based on the SFA results and was correlated with geological data.

3- GEOLOGICAL SETTING

3-1- Regional Geology

Milloieh copper deposit is situated in 80 km northeastern of Sirjan (SE Iran) and the Cenozoic Urumia-Dokhtar magmatic belt (Figure 1). Most of the Iranian Cu porphyry deposits occurred in the Cenozoic Urumieh-Dokhtar magmatic belt that is one of the subdivisions of Zagros orogenies [31-35], and are particularly revealed in the SE arc segment which is referred to as Kerman Cenozoic Magmatic Arc (KCMA) with 450 km length and 60-80 km width (Figure 1) [31,32]. The KCMA is located on the western boundary of the central Iranian block with calc-alkaline intrusive rocks (stocks) association [31].

According to exploratory studies, three major mineralization zones for this area has been considered. Milloieh (1), Milloieh (2), and Milloieh (3) zones which are located in western part of the area. Rock facies of Milloieh (1) and Milloieh (3) include dark porphyry andesite, while rock facies in Milloieh (2) are composed of light-colored tuff crystals. This deposit is located in the border section of Urmia-Dokhtar magmatic belt and ophiolitic zone in northeast of Sirjan (Figure 1). This region is situated in the volcano

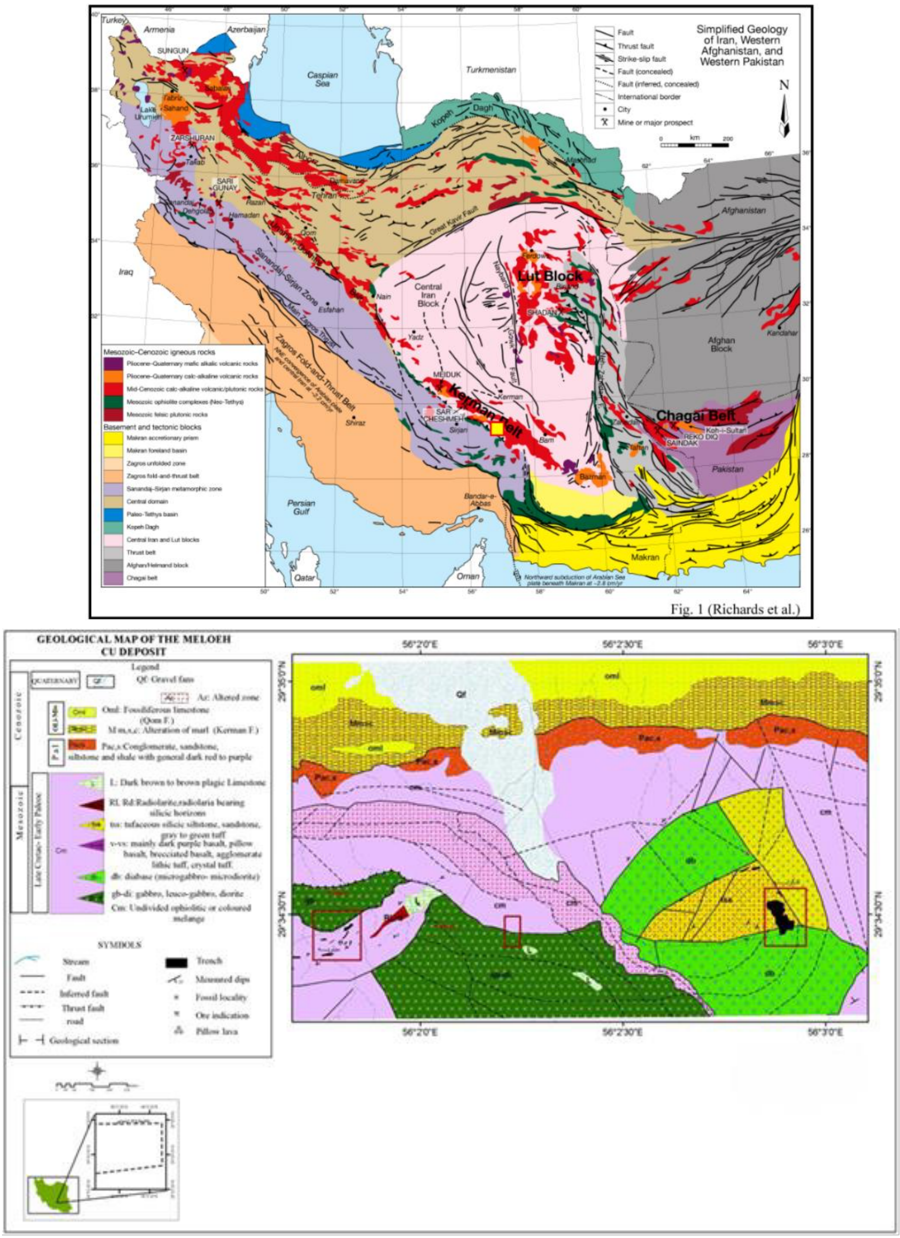

Figure 1. Location of Milloieh copper deposit (Yellow Square) on the map of Iran structural zones [35] and Geological map of Milloieh Area, scale: 1:10,000

plutonic part of Urmia-Dokhtar belt. The Urmia-Dokhtar magmatic belt is one of the main areas of copper mineralization in the world and it is a part of Himalaya-Alp orogenic belt. The most important feature of this magmatic belt is the presence of calc-alkaline intrusive masses which have penetrated from Oligocene to Miocene of volcanic units. Porphyric volcanic rocks include andesite and latite-andesite. Moreover, pyroclastic units are tuff, shale-tuff and crystalline tuffs. Many of these intrusive masses with porphyry texture have copper-molybdenum mineralization. There are intrusives with composition of quart diorite to diorite in the studied deposit.

3-2- Mineralization and Alteration

Mineralization in the KCMA occurred in quartz stockworks, veins and as spread sulfides in both the host stock and surrounding older volcanic and pyroclastic rocks [34,35]. Hypogene and supergene zones are existed in the Milloieh deposit.

Hydrothermal alteration at Milloieh is distinguished by a phyllic alteration and zones of propylitic, argillic and carbonate assemblages. Copper mineralization in the deposit is associated mainly with phyllic alteration zone. Hypogene ores at the Milloieh includes pyrite, chalcopyrite and minor magnetite and molybdenite. Moreover, there are covellite chalcocite, and rarely bornite in the supergene zone (Figure 2). Malachite, azurite, cuprite, goethite and iron oxides occurred in several surficial parts of the studied area.

4- DISCUSSION

From the seven drilled boreholes, 84 rock samples were collected and analyzed by ICP-AES for Cu, Mo and other 24 related elements by Zarazma Company. Distribution of Cu and Mo were not normal, as depicted in Figure 3. Detection limits for Cu and Mo are 1 ppm and 0.5 ppm. In this study, 8 samples were analysed as duplicate samples. Fisher test was carried out based on variances for quality control (Qc) and quality accuracy (Qa). However, mean value for Cu and Mo are 0.24% and 1.4 ppm, respectively. There are abnormal distributions for both of them.

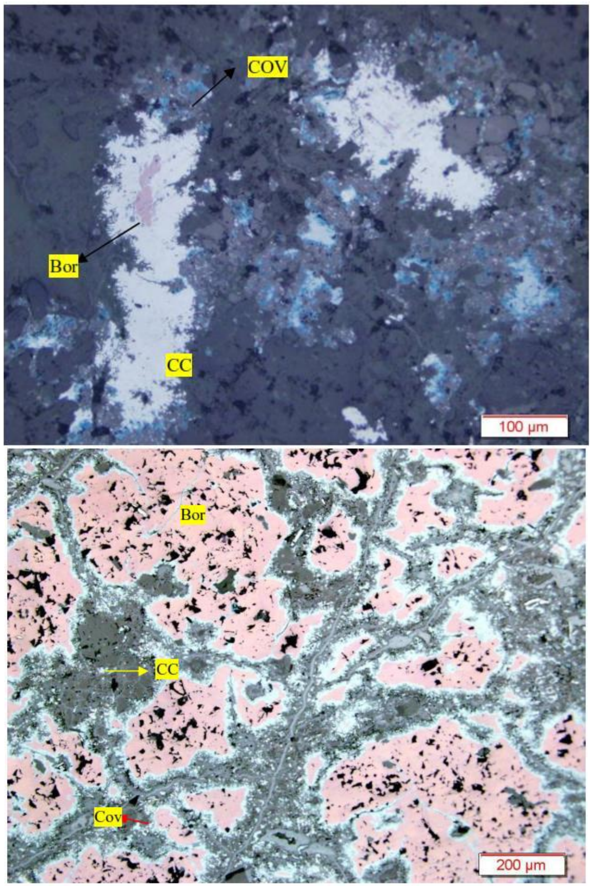

Figure 2. Two polished section from supergene enrichment zone (CC: Chalcocite; Bor: Bornite; COV: Covelite)

4-1- Application of the SFA

In factor analysis, a threshold value for the minimum loading criterion for elemental variables should be selected between the ranges of 0.3 to 0.6. Consequently, the absolute value of 0.5 is a medium loading value [12,13]. In this study, 0.6 was selected for the minimum loading criterion. The classical principal factor analysis for extracting the common factors was applied within varimax method [13] for rotation and retained factors with eigenvalues of >1 for interpretation and used the SFA and achieved stages to extract clean factor (common and more existing elements) of the Milloieh deposit. In the first stage of factor analysis, all elements were grouped in the six factors. Factors with index element of copper porphyry deposits were separated for second stages. Factors 2 and 4 include minor and ore elements which are Pb-S-Mn and Cu-Mo-Zn,

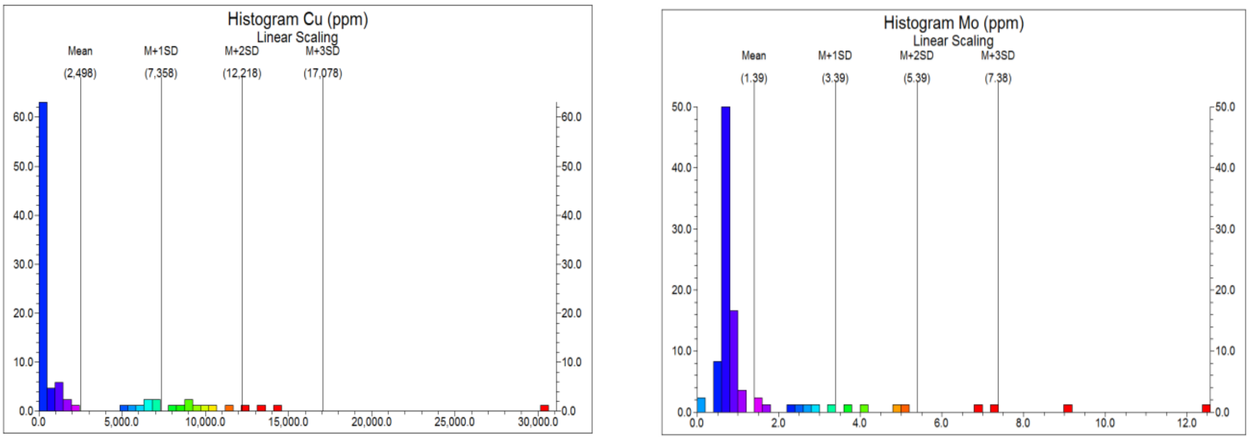

Figure 3. Histograms for Cu and Mo which show abnormal distribution

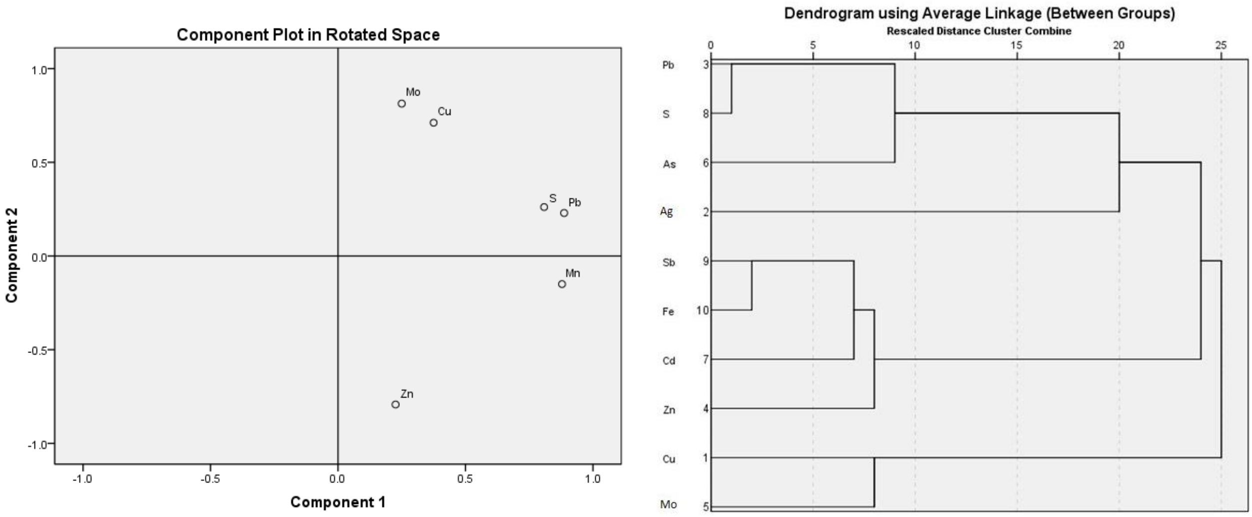

(A) (B)

Figure 4. A: Loading plot in the second stage of the SFA that shows F2-2 as main factor of mineralization in this area; and B: Dendrogram by cluster analysis

respectively. The second stage of factor analysis was executed on the index elements for to build new factors (Table 1). Finally, these remaining elements were separated in two groups including F1-2 (Pb, S and Mn) and F2-2 (Cu, Mo and Zn), as depicted in Table 1. Loading plot for second stage represents that the Cu and Mo are grouped to each other (Figure 4). In addition, cluster analysis was carried out based on R-mode method, as depicted in Figure 4. There are three clusters as follows:

1. Pb-S-As-Ag
2. Fe-Sb-Cd-Zn
3. Cu-Mo

The result is similar to the SFA technique. Cu and Mo exist in the third cluster such as F2-2.

4-2- Application of N-S Fractal Modelling

The F2-2 was selected for the N-S fractal modelling. Threshold values of F2-2 were determined in the N-S log-log plot, as depicted in Figure 5. There are two breakpoints and three populations for F2-2 (Cu and Mo). Supergene enrichment and hypogene zones are existed with F2-2 values >1.95 and 0.4-1.95, respectively.

Table 1. Two stages of the SFA in the Milloieh deposit (bold digits show factor scores higher than 0.6)

Rotated Component Matrix in first stage						
	Component					
	1	2	3	4	5	6
Ag	0.028	0.288	0.187	0.131	0.103	0.787
Ca	0.082	0.375	0.113	0.001	0.068	-0.785
Co	0.838	-0.186	0.222	0.018	0.050	0.000
Cr	0.813	-0.131	-0.120	-0.096	0.307	-0.266
Cu	-0.229	0.383	0.036	0.523	-0.053	0.488
Fe	0.803	-0.095	0.392	0.144	-0.039	0.163
Li	0.776	0.089	0.211	-0.305	-0.102	0.106
Mg	0.675	-0.069	-0.035	-0.173	0.640	-0.059
Mn	0.116	0.868	0.227	-0.185	0.017	-0.077
Mo	0.065	0.307	-0.004	0.779	0.051	0.256
Ni	0.744	0.307	-0.182	-0.056	0.131	-0.312
P	0.055	0.216	0.670	-0.007	0.601	0.083
Pb	-0.166	0.865	-0.095	0.209	-0.143	0.025
S	-0.297	0.805	0.117	0.150	0.135	0.089
Sb	0.400	-0.189	0.766	0.106	-0.033	-0.013
Sc	0.822	-0.236	0.145	0.083	0.142	-0.013
V	0.130	-0.028	0.076	0.157	0.926	0.015
Y	0.074	0.393	0.824	0.113	0.071	0.063
Zn	0.076	0.150	-0.168	-0.830	-0.066	0.079

Rotated Component Matrix in second stage		
	Component	
	1	2
Cu	0.375	0.711
Mn	0.878	-0.150
Mo	0.250	0.813
Pb	0.887	0.230
S	0.808	0.261
Zn	0.226	-0.793

5- CORRELATION BETWEEN RESULTS OBTAINED FROM N-S FRACTAL, SFA AND MINERALOGRAPHICAL CHARACTERISTICS

In this stage, the results generated by the SFA and fractal model are controlled by mineralogical investigations of core logging and polished section microscopic studies. Carranza provided a method for calculation of overlap correlations between two datasets [36]. An intersection operation between results from the SFA and fractal model and index minerals of different zones was performed to obtain numbers of samples corresponding to each of the four classes of overlap zones as represented in Table 2. Applied the obtained numbers of voxels, Type I error (T1E), Type II error (T2E), and overall accuracy (OA) of the fractal model were calculated with respect to the zonation model.

Correlation between the results obtained by the N-S fractal model and the index minerals

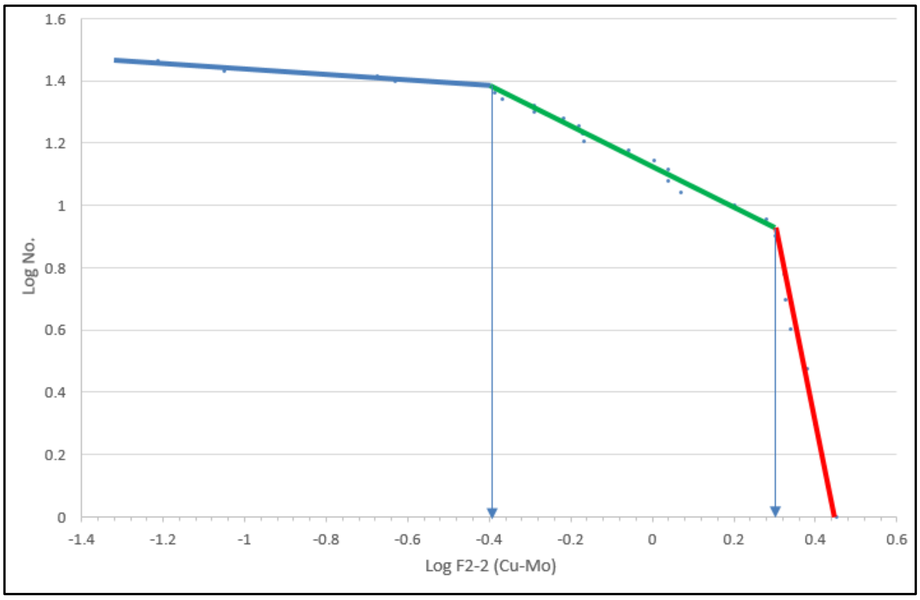

Figure 5. Log-log plot for F2-2 with three populations (Red and green populations are supergene enrichment and hypogene zones

Table 2. Matrix for comparing performance of fractal modeling results with geological model (A, B, C, and D represent numbers of samples in overlaps between classes in the binary datasets [36])

		Mineralographical data	
		Inside zone	Outside zone
SFA and fractal results	Inside zone	True positive (A)	False positive (B)
	Outside zone	False negative (C)	True negative (D)
		Type I error C/(A+C)	Type II error B/(B+D)
		Overall accuracy= (A+D)/(A+B+C+D)	

Table 3. OA, T1E and T2E, resulted from mineralographical data and supergene mineralized zone obtained through N-S fractal modelling of F2-2 data

		Supergene index mineral samples	
		Inside zone	Outside zone
SFA and fractal model of supergene zone	Inside zone	8	4
	Outside zone	7	65
		0.46	0.0579
		0.87	

of supergene enrichment zone (chalcocite, covellite and bornite) indicate that the supergene enrichment zone has more OA (0.87; Table 3). In addition, OA of the hypogene mineralized zone is 0.83, as depicted in Table 4. Average value for Cu and Mo are 0.86% and 5.3 ppm in supergene zone and also, mean of Cu and Mo in resulted hypogene zone are 0.59% and 1.88 ppm, respectively.

Table 4. OA, T1E and T2E, resulted from mineralographical data and hypogene mineralized zone obtained through N-S fractal modelling of F2-2 data

		Geological model (Zonation)	
		Inside zone	Outside zone
SFA and fractal model of hypogene zone	Inside zone	16	8
	Outside zone	12	54
		0.4	0.13
		0.83	

6- CONCLUSIONS

Results obtained by combination of the N-S fractal modelling and SFA show that the hybrid method is proper for delineation of various mineralized zones in the porphyry deposit based on multi-elemental data. The supergene enrichment zone contains F2-2≥ 1.96, Cu and Mo mean values are 0.86% and 5.3 ppm, respectively. Moreover, different mineralized zones can be recognized via the N-S fractal modelling and FSA. This method is applicable to results of factor analysis in different multi-elemental porphyry deposits such as Cu-Mo or Cu-Au for which the spatial patterns of concentration values satisfy a fractal model.

The supergene and hypogene zones detected via the SFA and C-V fractal model are correlated with mineralographical data due to application of logratio matrix. Based on the OAs, the overlapping between results obtained by the SFA and N-S fractal modelling with ore data are higher than 80% which shows that the hybrid method is proper for outlining of mineralized zones in the porphyry deposits.

7- References

[1] Berger, Byron R., Ayuso, Robert A., Wynn, Jeffrey C., Seal, and Robert R. (2008). *"Preliminary Model of Porphyry Copper Deposits"*. USGS, New York, pp. 55.

[2] Afzal, P., Yousefi, M., Mirzaei, M., Ghadiri-Sufi, E., Ghasemzadeh, S., and Daneshvar Saein, L. (2019). *"Delineation of podiform-type chromite mineralization using Geochemical Mineralization Prospectivity Index (GMPI) and staged factor analysis in Balvard area (southern Iran)"*. Journal of Mining and Environment, 10: 705-715.

[3] Cox, D., and Singer, D. (1986). *"Mineral deposits models"*. U.S Geological Survey Bulletin, pp. 1693.

[4] Shafiei, B., Haschke, M., and Shahabpour, J. (2009). *"Recycling of orogenic arc crust triggers porphyry Cu mineralization in Kerman Cenozoic arc rocks, southeastern Iran, Miner"*. Deposita, 44: 265-283.

[5] Daneshvar Saein, L. (2017). *"Delineation of enriched zones of Mo, Cu and Re by concentration-volume fractal model in Nowchun Mo-Cu porphyry deposit, SE Iran"*. Iranian Journal Earth Sciences, 9: 64-72.

[6] Afzal, P., Adib, A., and Ebadati, N. (2018). *"Delineation of seismic zonation using fractal modeling in West Yazd province, Central Iran"*. Journal of Seismology, 22(6): 1377-1393.

[7] Afzal, P., Fadakar Alghalandis, Y., Khakzad, A., Moarefvand, P., and Rashidnejad Omran, N. (2011). *"Delineation of mineralization zones in porphyry Cu deposits by fractal concentration-volume modeling"*. Journal of Geochemical Exploration, 108: 220-232.

[8] Afzal, P., Ghasempour, R., Mokhtari, A. R., and Asadi Haroni, H. (2015). *"Application of concentration-number and concentration-volume fractal models to recognize mineralized zones in North Anomaly iron ore deposit, Central Iran"*. Archives of Mining Sciences, 60: 777-789.

[9] Afzal, P., Mirzaei, M., Yousefi, M., Adib, A., Khalajmasoumi, M., Zia Zarifi, A., Foster, P., and Yasrebi, A. B. (2016). *"Delineation of geochemical anomalies based on stream sediment data utilizing fractal modeling and staged factor analysis"*. Journal of African Earth Sciences, 119: 139-149.

[10] Li, C., Ma, T., and Shi, J. (2003). *"Application of a fractal method relating concentrations and distances for separation of geochemical anomalies from background"*. Journal of Geochemical Exploration 77: 167-175.

[11] Treiblmaier, H., and Filzmoser, P. (2010). *"Exploratory factor analysis revisited: how robust methods support the detection of hidden multivariate data structures in IS research"*. Information and Management, 47: 197-207.

[12] Yousefi, M., Kamkar-Rouhani, A., and Carranza, E. J. M. (2012). *"Geochemical mineralization probability index (GMPI): A new approach to generate enhanced stream sediment geochemical evidential map for increasing probability of success in mineral potential mapping"*. Journal of Geochemical Exploration, 115: 24-35.

[13] Yousefi, M., Kamkar-Rouhani, A., and Carranza, E. J. M. (2014). *"Application of staged factor analysis and logistic function to create a fuzzy stream sediment geochemical evidence layer for mineral prospectivity mapping"*. Geochemistry: Exploration, Environment, Analysis (2014) 14 (1): 45–58.

[14] Shahsavar, S., Jafari Rad, A. R., Afzal, P., and Nezafati, N. (2020). *"Selection of Optimum Fractal Model for Detection of Stream Sediments Anomalies"*. Geopersia, 10: 395-404.

[15] Zamyad, M., Afzal, P., Pourkermani, M., Nouri, R., and Jafari, M. R. (2019). *"Determination of Hydrothermal Alteration Zones by Remote Sensing Methods in Tirka Area, Toroud, NE Iran"*. Journal of the Indian Society of Remote Sensing, 47: 1817-1830.

[16] Zuo, R., Agterberg, F. P., Cheng, Q., and Yao, L. (2009). *"Fractal characterization of the spatial distribution of geological point processes"*. International Journal of Applied Earth Observation and Geoinformation, 11(6): 394-402.

[17] Agterberg, F. P. (1995). *"Multifractal modeling of the sizes and grades of giant and supergiant deposits"*. International Geology Review, 37: 1-8.

[18] Nazarpour, A. (2018). *"Application of C-A fractal model and exploratory data analysis (EDA) to delineate geochemical anomalies in the: Takab 1:25,000 geochemical sheet, NW Iran"*. Journal of Earth Sciences, 10: 173-180.

[19] Shahsavar, S., Jafari Rad, A., Afzal, P., Nezafati, N., and Akhavan Aghdam, M. (2019). *"Prospecting for polymetallic mineralization using step-wise weight assessment ratio analysis (SWARA) and fractal modeling in Aghkand Area, NW Iran"*. Arabian Journal of Geosciences, 12(7): 248-257.

[20] Cheng, Q., Agterberg, F. P., and Ballantyne, S. B. (1994). *"The separation of geochemical anomalies from background by fractal methods"*. Journal of Geochemical Exploration, 51: 109-130.

[21] Mandelbrot, B. B. (1983). *"The fractal geometry of nature"*. Freeman, W. H., San Fransisco, pp. 468.

[22] Hassanpour, S., and Afzal, P. (2013). *"Application of concentration–number (C–N) multifractal modeling for geochemical anomaly separation in Haftcheshmeh porphyry system, NW Iran"*. Arabian Journal of Geoscience, 6: 957-970.

[23] Davis, J. C. (2002). *"Statistics and data analysis in Geology"*. 3th Ed., John Wiley & Sons Inc., New York, pp. 656.

[24] Reimann, C., and Filzmoser, P. (2000). *"Normal and lognormal data distribution in geochemistry: Death of a myth. Consequences for the statistical treatment of geochemical and environmental data"*. Environmental Geology, 39: 1001-1014.

[25] Filzmoser, P., Hron, K., and Reimann, C. (2009). *"Principal components analysis for compositional data with outliers"*. Environmetrics, 20: 621-632.

[26] Fyzollahhi, N., Torshizian, H., Afzal, P., and Jafari, M. R. (2018). *"Determination of lithium prospects using fractal modeling and staged factor analysis in Torud region, NE Iran"*. Journal of Geochemical Exploration, 189: 2-10.

[27] Farahmandfar, Z., Jafari, M. R., Afzal, P., and Ashja Ardalan, A. (2020). *"Description of gold and copper anomalies using fractal and stepwise factor analysis according to stream sediments in NW Iran"*. Geopersia, 10(1): 135-148.

[28] Jebeli, M., Afzal, P., Pourkermani, M., and Jafarirad, A. R. (2018). *"Correlation between rock types and copper mineralization using fractal modeling in Kushk-e-Bahram deposit, Central Iran"*. Geopersia, 8(1): 131-141.

[29] Ostadhosseini, A., Barati, M., Afzal, P., and Lee, I. (2018). *"Polymetallic mineralization prospecting using fractal and staged factor analysis in Ardestan area, Central of Iran"*. Geopersia, 8: 279-292.

[30] Mirzaei, M., Afzal, P., Adib, A., Rahimi, E., and Mohammadi, Gh. (2020). *"Detection of zones based on ore and gangue using fractal and multivariate analysis in Chah Gaz iron ore deposit, Central Iran"*. Journal of Mining and Environment, 11(2): 453-466.

[31] Aghazadeh, M., Badrzadeh, Z., Hou, Z., and Zhou, L. (2015). *"Temporal-spatial distribution and tectonic setting of porphyry copper deposits in Iran: Constraints from zircon U-Pb and molybdenite Re-Os geochronology"*. Ore Geology Reviews, 70: 385-406.

[32] Alavi, M. (1994). *"Tectonic of Zagros orogenic belt of Iran: new data and interpretations"*. Tectonophysics, 229: 211-238.

[33] Aliyari, F., Afzal, P., Harati, H., and Zengqian, H. (2020). *"Geology, mineralogy, ore fluid characteristics, and 40Ar/39Ar geochronology of the Kahang Cu-(Mo) porphyry deposit, Urumieh-Dokhtar Magmatic Arc, Central Iran"*. Ore Geology Reviews, 1-25.

[34] Asadi, S., Moore, F., and Zarasvandi, A. (2014). *"Discriminating productive and barren porphyry copper deposits in the southeastern part of the central Iranian volcano-plutonic belt, Kerman region, Iran: A review"*. Earth-Science Reviews, 138: 25-46.

[35] Richards, J. P. (2015). *"Tectonic, magmatic, and metallogenic evolution of the Tethyan orogen: From subduction to collision"*. Ore Geology Reviews, 70: 323-345.

[36] Carranza, E. J. M. (2011). *"Analysis and mapping of geochemical anomalies using logratio-transformed stream sediment data with censored values"*. Journal of Geochemical Exploration, 110: 167-185.